Praise Worthy Prize

International Review of Electrical Engineering (I.R.E.E.), Vol. 7, N. 2
ISSN 1827- 6660 *March-April 2012*

Compensation of Wind Generator Power Fluctuations in Microgrid Applications by Superconducting Magnetic Energy Storage

Marcelo G. Molina, Gastón O. Suvire, Pedro E. Mercado

Abstract – *Grid connection of wind power generation (WPG) is becoming today an important form of distributed generation (DG). The penetration of these DG units into AC microgrids (MGs) is growing rapidly, enabling reaching high percentage of the installed generating capacity. However, the fluctuating and intermittent nature of this renewable generation causes variations of power flow that can bring both power quality and reliability issues to the electrical grid. To overcome these problems, superconducting magnetic energy storage (SMES) arises as a potential alternative to compensate these power flow fluctuations and thus to significantly enhance the MG dynamic security. To this aim, the management of the energy stored in the SMES device is crucial for optimizing the storage capacity as well as for preventing the device from becoming overcharged or uncharged. This paper proposes the use of an improved SMES controller for the stabilization of the fluctuating active power injected into the microgrid by wind generators. In this sense, the design and implementation of a high performance active power controller of the SMES is described. The control is based on fuzzy logic techniques and uses an enhanced fuzzy inference system (FIS) combined with a unique filter block. Moreover, a detailed model of the SMES unit and its power conditioning system (PCS) for connecting to the electric grid is derived. The dynamic performance of the proposed system and its impact on the MG operation is validated by computer simulation.*

Keywords: *Microgrid (MG), Distributed Generation (DG), Wind Generation, Superconducting Magnetic Energy Storage (SMES), Fuzzy Logic Controller (FLC), Detailed Modeling*

I. Introduction

In the last decade, power generation technology innovations and a changing economic, financial, and regulatory environment of the power markets have resulted in a renewed interest in on-site small-scale electricity generation, also called distributed, dispersed or decentralized generation (DG) [1]. Other major factors that have contributed to this evolution are the constraints on the construction of new transmission lines, the increased customer demand for highly reliable electricity and concerns about climate change [2]. Along with DG, local storage directly coupled to the grid (aka distributed energy storage or DES) is also assuming a major role for balancing supply and demand. All these distributed energy resources (DERs), i.e. DG and DES, are presently increasing their penetration in developed countries as a means to produce in-situ highly reliable and good quality electrical power [3].

Incorporating advanced technologies, sophisticated control strategies and integrated digital communications into the existing electricity grid results in Smart Grids (SGs), which are presently seen as the energy infrastructure of the future intelligent cities [4], [5].

Smart grids allow delivering electricity to consumers using two-way digital technology that enable the efficient management of consumers and the efficient use of the grid to identify and correct supply-demand imbalances. Smartness in integrated energy systems (IESs) which are called microgrids (MG) refers to the ability to control and manage energy consumption and production. In such IES systems, the grid-interactive AC microgrid is a novel network structure that allows obtaining the better use of DERs by operating a cluster of loads, DG and DES as a single controllable system with predictable generation and demand that provides both power and heat to its local area by using advanced equipments and control methods [6], [7]. This grid, which usually operates connected to the main power network but can be autonomously isolated (islanded) during an unacceptable power quality condition, is a new concept developed to cope with the integration of renewable energy sources (RESs) [8].

Grid connection of RESs, such as wind power generation (WPG), is becoming today an important form of DG [9]. The penetration of these DG units into AC-interactive microgrids is growing rapidly, enabling reaching high percentage of the installed generating

Manuscript received and revised March 2012, accepted April 2012

capacity. However, the fluctuating and intermittent nature of this renewable generation causes variations of power flow that can bring both power quality and reliability issues to the electrical grid [10]-[12]. This situation can lead to severe problems that dramatically jeopardize the microgrid security, such as system frequency oscillations, and/or violations of power lines capability margin, among others. This condition is worsened by to the low inertia present in the microgrid; thus requiring having available sufficient fast-acting spinning reserve.

To overcome these problems, superconducting magnetic energy storage (SMES) arises as a potential alternative in order to compensate these power flow fluctuations and thus to considerably augment the MG dynamic security [13]. With proper controllers, this advanced DES is capable of supplying the microgrid with both active and reactive power, simultaneously and very fast, and hence is able to provide the required security level.

To this aim, the management of the energy stored in the SMES device is essential for optimizing the storage capacity as well as for avoiding the device from becoming overcharged or uncharged. In this way, an efficient energy management function is needed, which can be implemented via a high-priority level active power controller of the SMES. This control strategy must achieve simultaneously two goals: one is to compensate the active power fluctuations injected into the microgrid by wind generators, and the other is to make an appropriate management of the stored energy.

Many solutions have been proposed and studied, particularly over the last decades, to compensate wind generator power fluctuations using SMES systems [14]-[18]. These papers addressing the control issues are focused mainly on the ability of the SMES to control the active or/and reactive power flow. However, much less has been done particularly on the utilization of SMES devices in emerging AC-interactive microgrids, although major benefits apply [19]-[21]. Moreover, none of these works have discussed the strategies to stabilize the active power flow of wind generators according to the SMES coil state-of-charge.

Based on the previous discussion, this paper proposes the use of an improved SMES controller for the stabilization of the fluctuating active power injected into the microgrid by wind generators. In this sense, the design and implementation of a novel high performance active power controller of the SMES is described. The control technique is based on fuzzy logic and uses an enhanced fuzzy inference system (FIS) combined with a unique filter block.

Moreover, a detailed model of the SMES unit and its power conditioning system (PCS) for connecting to the electric grid is derived. The dynamic performance of the proposed system and its impact on the MG operation is fully validated by computer simulation in the MATLAB/Simulink environment.

II. Modeling of the SMES System

A SMES system consists of several sub-systems, which must be carefully designed in order to obtain a high performance compensation device. The base of the SMES unit is a large superconducting coil (SC) with its filtering and protection system. On the other hand, the power conditioning system enables the grid-interactive operation of the SMES unit in both charge and discharge modes. This section briefly describes the proposed detailed model of the SMES system for applications in the distribution network level, which is shown in Fig. 1.

This model is comprehensively analyzed in [20], [22], including the design principles and implementation issues of the SMES and its power conditioning system.

II.1. Power Conditioning System

The PCS provides a power electronic interface between the SC and the point of common coupling (PCC) to the AC microgrid, aiming at achieving two goals: one is to convert electric power from DC to AC (with fixed voltage and frequency set by the utility grid), and the other is to charge/discharge efficiently the SC.

The proposed PCS allows meeting all the specific microgrid code requirements of power quality, flexibility, efficiency and reliability demanded to modern DG systems. The key part of the PCS is the well-known voltage source inverter (VSI), also called voltage source converter (VSC), which is built with semiconductor devices having turn-off capabilities. This electronic converter is shunt-connected to the distribution network by means of a step-up Δ–Y coupling transformer and the corresponding line sinusoidal filter, as described in Fig. 1 (right side). This grid-side inverter corresponds to a DC/AC static converter using high-power fast isolated gate bipolar transistors (IGBTs). In addition, the output voltage control of the VSI is achieved through sinusoidal pulse width modulation (SPWM) techniques [20]-[23].

The proposed inverter structure is based on a diode-clamped three-level twelve-pulse topology, aka neutral point clamped (NPC), instead of a standard two-level six-pulse inverter structure. This three-level twelve-pulse VSI topology allows generating at the PCC to the AC grid a set of three almost sinusoidal voltage waveforms at the fundamental frequency phase-shifted 120º between each other, with lesser harmonics distortion, better efficiency and faster dynamic response than conventional two-level structures without increasing the switching frequency and effectively doubles the power rating of the VSI for a given semiconductor device. Moreover, the three level pole attempts to address some limitations of the standard two-level by offering an additional flexibility of a level in the output voltage, which can be controlled in duration, either to vary the fundamental output voltage or to assist in the output waveform construction. This extra feature is used here to assist in the output waveform structure [22].

The inclusion of a SMES coil into the DC bus of the VSI demands the use of a rapid and robust bidirectional interface to adapt the wide range of variation in voltage and current levels between both devices. Controlling the SMES coil rate of charge/discharge requires varying as much the coil voltage magnitude as the polarity according to the coil state-of-charge, while keeping essentially constant and balanced the voltage of the VSI DC link capacitors. To this aim, a two-quadrant three-level IGBT DC/DC converter or chopper is proposed to be employed, as shown in Fig. 1 (middle side) [22]. This converter makes use of the extra level mainly to maintain the charge balance of the DC capacitors; thus avoiding introducing additional distortion into the microgrid and reducing switching losses and the VSI DC current ripple. Other advantage of this three-level DC/DC chopper topology compared to a traditional two-level one includes the reduction of voltage stress of each IGBT by half, permitting to increase the chopper power ratings while maintaining high dynamic performance. This step-down and step-up multi-level converter allows decreasing the ratings of the overall PCS (specifically the VSI and the transformer) by regulating the current flowing from the SMES coil to the inverter of the VSI and vice versa.

II.2. SMES Coil

The base of the SMES unit is a superconducting coil, whose basic structure is composed of the cold components itself (the SC with its support and connection components, and the cryostat) and the cryogenic refrigerating system [23].

The equivalent circuit of the SMES coil makes use of a lumped parameters network represented by a six-segment model comprising self inductances (L_i), mutual couplings between segments (i and j, M_{ij}), AC loss resistances (R_{si}), skin effect-related resistances (R_{pi}), turn-ground (shunt–C_{Shi}) and turn-turn capacitances (series–C_{Si}), as depicted at the left side of Fig. 1. This model is based on the ones previously proposed in [24], and is reasonably accurate for electric system transients' studies, over a frequency range from DC to several thousand Hertz. The inclusion of surge capacitors (C_{Sg1} and C_{Sg2}) and a filter capacitor C_F in parallel with grounding-balance resistors (R_{g1} and R_{g2}) allows reducing the effect of resonances. A metal oxide semiconductor (MOV) protection for transient voltage surge suppression is included between the SMES model and the DC/DC converter.

III. Proposed Control Scheme of the SMES

The proposed hierarchical control scheme of the SMES unit consists of an external, middle and internal level. Its design is performed in the synchronous-rotating *d-q* reference frame [25]. This structure has the goal of rapidly and simultaneously controlling the active and reactive power flow provided by the SMES. To this aim, the controller must ensure the instantaneous energy balance among all the SMES components. In this way, the stored energy is regulated through the PCS in a controlled manner for achieving the charging and discharging of the SC coil.

III.1. External Level Control

The external level control, which is outlined in Fig. 2 (left side), is responsible for determining the active and reactive power exchange between the SMES and the AC microgrid. The control strategy applied can be designed to perform various control objectives with different priorities. The power set-points are either specified based on a general power dispatch strategy via a supervisory power management or a locally calculated active/reactive power compensation of the load or the MG feeder. In this paper, the control system is designed to achieve two major high-priority control objectives: the voltage control mode (VCM) with only reactive power compensation capabilities (no energy storage is required), and the active power control mode (APCM) with active power exchange capabilities aiming at compensating the active power fluctuations injected into the AC microgrid by wind generators, while providing an adequate management of the energy stored in the superconducting coil; thereby avoiding that the SMES becomes overcharged or uncharged. In normal grid-connected operation mode of the microgrid, the APCM of the SMES is an essential management function rather than the frequency and voltage control, which are crucial for islanded mode.

In this level, the instantaneous voltage at the SMES PCC to the microgrid is computed by employing a synchronous-rotating reference frame. Thus, by applying Park's transformation, the instantaneous values of the three-phase AC bus voltages are transformed into *d-q* components, v_d and v_q respectively. By defining the *d*-axis always coincident with the instantaneous voltage vector v, then v_d results in steady-state equal to $|v|$ while v_q is null. Consequently, the *d*-axis current component of the VSI contributes to the instantaneous active power p while the q-axis current component represents the instantaneous reactive power q, as explained in [22]. Additionally, the instantaneous actual output currents of the SMES, i_d and i_q, are computed for use in the middle level control. A phase locked loop (PLL) is used to synchronize, through the phase θ_s, the coordinate transformations from *abc* to *dq* components in the voltage and current measurement system. The phase signal is derived from the positive sequence components of the AC voltage vector measured at the PCC of the SMES.

The standard control block of major emerging distributed energy resources (DG or DES) is the VCM and consists in a voltage-droop strategy used to modulate

the reactive component of the VSI output current, i_q aiming at controlling the voltage at the PCC of the SMES to the MG distribution feeder. This control mode has proved a very good performance in conventional static var compensators (with no energy storage). As can be noted, the energy storage feature of the SMES is not utilized in this operation mode, and the power inverter itself generates electronically the required reactive power. This reactive power control loop employs a standard proportional-integral (PI) controller with a voltage droop characteristic (becoming the phase-lag compensator LC_1) for enabling a stable fast-response operation with more DERs or static var compensators operating in the area. This characteristic is comparable to the one included in conventional generators´ voltage regulators [26]. The APCM is the dominant control mode which aims at controlling the active power exchanged with the MG with the goal of stabilizing (smoothing or even fully eliminating) the fluctuating power injected by wind generators. This objective is basically achieved by controlling the direct component of the SMES VSI output current, i_d in a way that the SMES coil is forced to absorb active power from the MG PCC when P_r is negative (charge mode), or to inject active power when P_r is positive (discharge mode).

In this case, the reference of the SMES device output direct current, i_{dr} is straightforwardly derived from the novel proposed active power controller via a conventional proportional-integral (PI) block, in concordance with the active power wind generation, P_{wg}.

Furthermore, the state-of-charge of the SMES is constantly monitored in order to provide a suitable management of the energy stored in the superconducting coil by means of the active power controller.

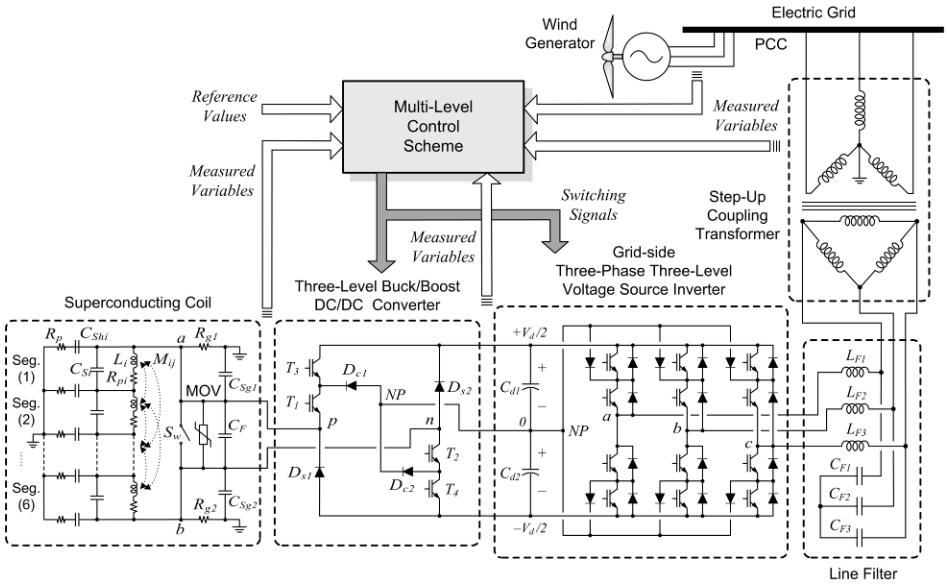

Fig. 1. Detailed model of the proposed SMES system, including the superconducting coil and its power conditioning system

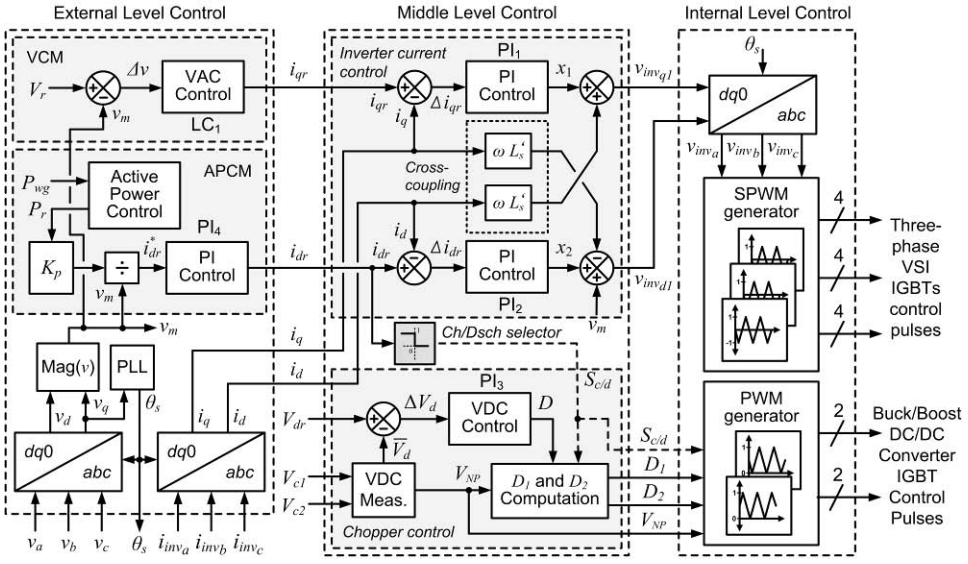

Fig. 2. General structure of the multilevel level control of the SMES system

Fig. 3 shows a basic structure of the active power controller. This controller architecture is designed on the basis of a fuzzy logic controller (FLC), and uses an enhanced fuzzy inference system (FIS) [27] combined with a unique filter block that allows tracking the wind generation in very short times with respect to the SC state-of-charge.

The purpose of the FIS is to estimate the value of a regulating power, P_{reg}, which correspond to the power required to supply the AC microgrid (i.e. the wind generator plus the SMES device). The difference between the regulating power, P_{reg}, and the power injected by wind generator, P_{wg} is the reference power, P_r, which must be either stored or delivered by the SMES system.

The SMES coil current, I_{SC} has a finite range of variation; therefore, the active power controller must adapt the value of regulating power as a function of the wind power generation and the superconducting coil current. The controller inputs are the corrected value of wind power generation, $P_{wg\text{-}c}$ and SMES coil current, I_{SC}, which measures the state-of-charge of the energy storage device. The corrected power of wind generation, $P_{wg\text{-}c}$ is calculated from the wind power generation, P_{wg} after being smoothed by a special filter consisting of a backlash block and a second-order low-pass filter.

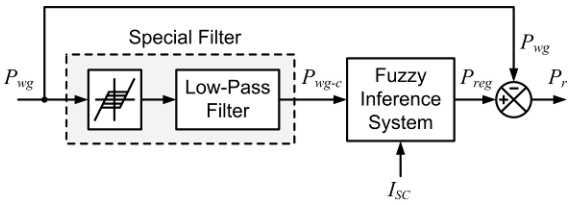

Fig. 3. Basic structure of the active power controller

The backlash block implements a system where an input change causes an equal output change. However, when the input changes direction, an initial input change has no effect on the output. The amount of side-to-side play in the system is referred to as the dead-band (DB), and it is centered about the output [28].

The backlash system can be in one of three modes:

- Disengaged: In this mode, the input does not drive the output and the output remains constant.
- Engaged in a positive direction: In this mode, the input is increasing (i.e., it has a positive slope) and the output is equal to the input minus half the DB width.
- Engaged in a negative direction: In this mode, the input is decreasing (i.e., it has a negative slope) and the output is equal to the input plus half the DB width.

Figs. 4 illustrate the operation of the backlash system. Fig. 4(a) shows the relationship between the input and the output while the system is in disengaged mode. Fig. 4(b) shows the state of the block when the input has reached the end of the DB and engaged the output. In this way, the output remains in its previous value. Finally, Fig. 4(c) shows how a change in the input affects the output while the system is engaged.

If the input reverses its direction, it disengages from the output. The output remains constant until the input either reaches the opposite end of the dead-band or reverses its direction again and engages at the same end of the dead-band.

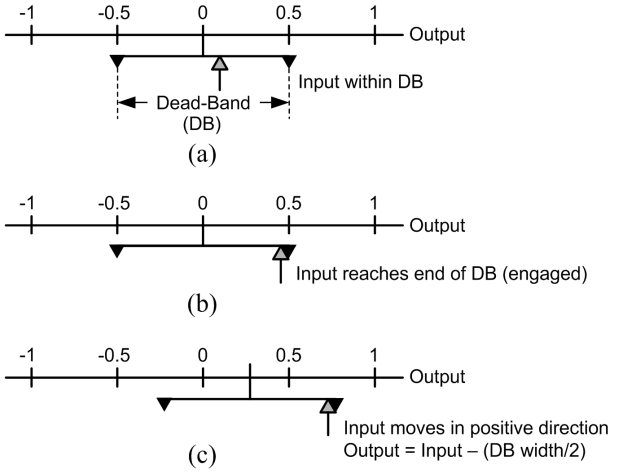

Figs. 4. Operation of the backlash system

The filter block implements a simple fixed-gain second-order low-pass filter using a Sallen-Key topology to make smoother changes of output of the backlash system.

The fuzzy logic controller proposed for this application is based on the following principles [29]:

- If the SMES coil current, I_{SC} is too low, then the energy storage will be benefited. A larger amount of power produced by the wind generator is used to charge the superconducting coil and, consequently, less power is supplied to the microgrid from the combined wind generator-SMES device.
- If the superconducting coil current is too high, then the power generation will be benefited. A larger amount of wind generator power is supplied to the microgrid, therefore less power is stored into the SMES.
- If the SMES coil current is such that the stored energy is half the maximum usable one, then the system is under normal operation. In this condition, neither power generation nor storage is benefited. The electric grid is provided with wind power generation with fluctuations smoothed by the energy storage device.

The input variables to the FIS block are the corrected wind power generation, $P_{wg\text{-}c}$ and SMES coil current, I_{SC}.

The first input is in per unit values (p.u.) which varies between 0 and 1, whereas the second input varies between the operating limits of the SMES. This admissible operating range of the SMES coil is limited by the maximum rate of change in the SC without violating the superconductivity of the device (maximum SC current) and the minimum operating current which

assures the continuous current conduction mode of the DC/DC converter, which can be usually assumed at 20% of maximum rating [15].

For these input variables, five fuzzy sets are considered: Low (L), Low Medium (LM), Medium (M), High Medium (HM) and High (H).

The output variable of the FIS is the regulating power, P_{reg}, which is divided into seven linguistic values: Very Low (VL), Low (L), Low Medium (LM), Medium (M), High Medium (HM), High (H) and Very High (VH).

Fuzzy values are mapped via membership functions, both to the input variables and to the output variables. After a thorough selection based on analyzing the results of simulations with different membership functions (triangular, trapezoidal and Gaussian), the triangular fuzzy sets have been chosen for simplicity. The membership functions of the input and output variables are presented in Figs. 5.

The membership functions of the first input ($P_{wg\text{-}c}$) and the output (P_{reg}) have been distributed proportionally along the universe of discourse of each variable. The membership function of the second input (I_{SC}), which represents the state-of-charge of the energy storage, has been distributed with different forms for the triangles.

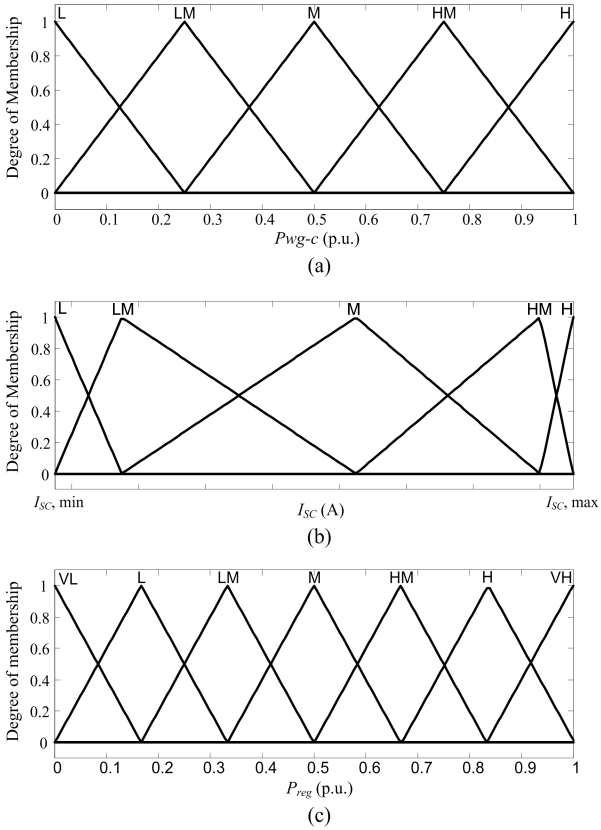

Figs. 5. Membership functions of input and output variables: (a) Corrected wind power generation, $P_{wg\text{-}c}$. (b) SMES coil current, I_{SC}. (c) Regulating power, P_{reg}

After testing different distributions for the triangles of this input, the one shown in Fig. 6 was chosen since these distributions yielded better results (the compensation of wind power fluctuations, both smoothly and without sudden changes, was achieved).

For the FIS implemented in this work, the fuzzy rules are determined from Table I. This table is created based on the principles previously mentioned, which aims at smoothing the wind power fluctuations and making a suitable management of the energy stored in the SMES.

TABLE I
INFERENCE TABLE TO OBTAIN THE OUTPUT P_{reg}

		I_{SC}				
		L	**LM**	**M**	**HM**	**H**
$P_{wg\text{-}c}$	**L**	VL	VL	L	LM	M
	LM	VL	L	LM	M	HM
	M	L	LM	M	HM	H
	HM	LM	M	HM	H	VH
	H	M	HM	H	VH	VH

In this application, a Mamdani-type fuzzy inference system is implemented [29]. In addition, the defuzzyfication strategy applied is the fuzzy mean method [30]. The output of the FIS ranges from 0 to 1.

The evolution of the regulating power, P_{reg} versus the superconducting coil current, I_{SC} and the corrected wind power generation, $P_{wg\text{-}c}$ is shown in Fig. 6.

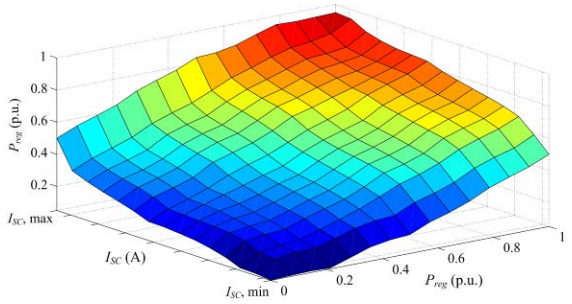

Fig. 6. P_{reg} versus I_{SC} and $P_{wg\text{-}c}$, obtained with the proposed FIS

III.2. Middle Level Control

The middle level control makes the expected output, i.e. the VSI output currents i_d and i_q, to dynamically track the reference values set by the external level (i_{dr} and i_{qr}). The middle level control design (shown in Fig. 2, middle side), implements a full decoupled current control strategy of the inverter in the synchronous-rotating *dq* reference frame. To this aim, a linearization of the state-space averaged model of the VSI in *d-q* coordinates is employed, which is described in-depth in [22]. In order to achieve a fully decoupled active and reactive power control, it is required to decouple the *d-* and *q-axis* current controls through two conventional PI controllers (PI_1 and PI_2) and voltage cross-coupling elimination feed-forward terms. In addition, another PI controller (PI_3) is required in order to eliminate the extra coupling resulting from the DC capacitors voltage V_d ($V_{c1}+V_{c2}$) as much in the DC side as in the AC side of the inverter. This is achieved with a DC voltage control using the DC/DC chopper in order to eliminate the steady-state voltage variations at the DC bus, by forcing the

instantaneous balance of power between the DC and the AC sides of the PCS inverter. Thus, this control loop is designed for computing the duty cycle D of the chopper semiconductors for the required stiff voltage at the DC bus according to the mode of operation of the DC/DC converter (charge/discharge). A charge/discharge (*Ch/Dsch*) selection block is used to set the operation of the converter through the signal $S_{c/d}$, and duty cycles D_1 and D_2 are computed through a dedicated controller in order to balance the DC bus capacitors voltage by managing the redundant switching states of the chopper according to the capacitors charge unbalance measured through the neutral point voltage, V_{NP}.

III.3. Internal Level Control

Fig. 2 (right side) shows a basic scheme of the internal level control of the SMES unit. The internal level provides dynamic control of input signals for the DC/AC and DC/DC converters from the output reference signals determined by the middle level control. This level is responsible for generating the triggering control signals for the twelve valves of the three-level VSI, according to the modulation techniques (SPWM) and types of semiconductors (IGBTs) used, and for the four IGBTs of the buck/boost three-level DC/DC converter.

In the case of the sinusoidal PWM pulses generator block, the controller of the VSI generates pulses for the carrier-based three-phase PWM inverter using the three-level topology. Thus, the expected sinusoidal-based output voltage waveform v_{inv} of the SMES is derived from the coordinate transformation from *dq* components provided by the middle level control by producing three-state SPWM vectors. These states are decoded by the states-to-pulses decoder for obtaining the firing pulse for each IGBT of the four ones in each leg of the three-phase three-level VSI.

In the case of the DC/DC converter firing pulses generator block, the three-level PWM modulator is built using a compound signal obtained as the difference of two standard two-level PWM signals. According to the mode of operation of the chopper (charge/discharge), the consequent three-state PWM vectors are synthesized for relating each state with the corresponding firing pulse for each IGBT of the four ones in each leg of the three-level DC/DC converter. The selection of the appropriate states that command the chopper is a function of the DC bus voltage unbalance measured through V_{NP} and hence of the contribution of charge from capacitors C_{d1} and C_{d2}.

IV. Digital Simulation Results

The test power system used to validate the proposed full detailed modeling and control methodologies of the SMES device for smoothing the wind power fluctuations in MG applications and making a suitable management of the energy stored in the SMES is depicted in Fig. 7 as a single-line diagram. This electric power network implements a bulk power system providing a small AC microgrid, which includes a variety of DER units (DG based on fossil and renewable fuels and the advanced SMES) and different types of loads (DR).

The small grid-interactive AC microgrid implements a dynamically-modeled single generator-type DG linked to a bulk utility system represented by a classical single machine-infinite bus type (SMIB) system [20]. The first microgenerator is composed of a dispatchable unit powered by a gas microturbine and includes a voltage regulator and a speed governor. The second generator is made up of a variable speed wind turbine generator implemented with a direct-in-line PMSG grid-tied via a full-scale power converter.

The test MG implements an automatic load frequency control. This basic 13-bus network operates at 120 kV/50 Hz in the bulk system side (main grid) and at 25 kV in the microgrid side, and implements a 100 MVA short circuit power level infinite bus through a Thevenin equivalent. Two sets of sheddable linear loads, grouped respectively at buses 10 and 11, are modeled as constant impedances. A microgrid central breaker (MGCB) with automatic reclosing capabilities is employed for the interconnection of the microgrid PCC (also called PCC-MG or bus 5) to the bulk power network through a 20 km tie-line. This high-speed grid separation device is implemented via a solid state circuit breaker (static transfer switch), and is used to rapidly disconnect the MG from the faulted bus in case of an unacceptable power quality condition.

The proposed SMES device representing the microgrid DES is placed at bus 6, which corresponds to the PCC of the wind generator to the rest of the MG, and includes a 25 kV/1.2 kV step-up transformer with a ±2 MVA/2.5 kV DC bus PCS and a 1 MW/27 MJ SMES device. The SMES system is composed of a stack of 4 high temperature superconductor (abbreviated high-T_c or simply HTS) coils with a total equivalent nominal inductance of 28 H per stack operated at 30 K (T_c), and a critical global current $I_{sc,\,max}$ of 1.2 kA. The minimum operating SMES current $I_{sc,\,max}$ is assumed at 20% of maximum rating, i.e. approximately 283.4 A. Major data of the proposed test power system are provided in the Appendix of [20].

The dynamic performance of the proposed SMES device in smoothing the power fluctuations injected into the MG by the wind generator is assessed through digital simulations carried out in the MATLAB/Simulink environment [31], by using SimPowerSystems and C++ codes. To this aim, the SMES system is firstly charged to be initialized at half the operating capacity of 27 MJ, i.e. at about 13.5 MJ, so that the consequent initial coil current I_{sc} is set at about 1022 A, and then the system is set at the stand-by mode. Thus, the most important control mode of the SMES device in grid-interactive operation, i.e. the APCM, is analyzed considering two case studies which represent simple events that impose high demands upon the dynamic response of the device.

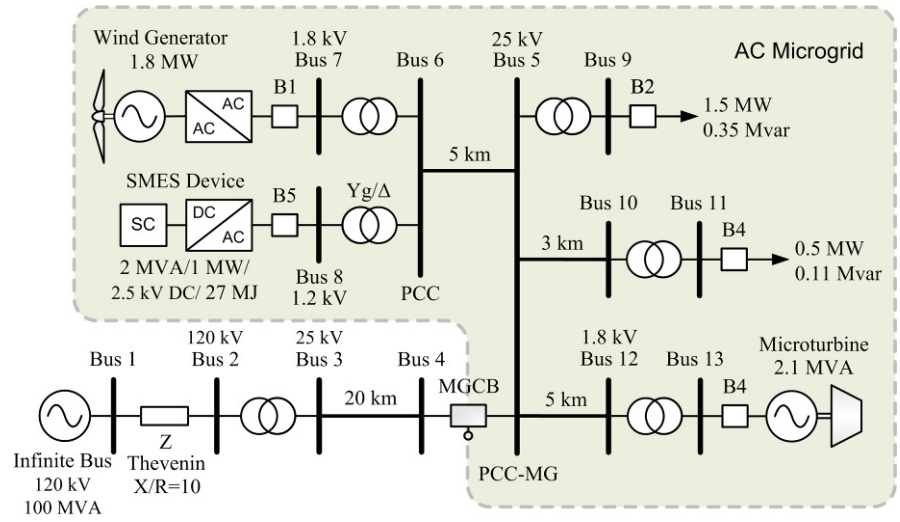

Fig. 7. Single-line diagram of the test power system with an AC microgrid including wind generation and the SMES system

The first case study (Scenario 1) discusses the performance of the proposed FIS control scheme of the SMES device in comparison with another efficient control presented in the literature [20]. In the second case study (Scenario 2), simulations are made considering different storage capacities of the SMES system with the proposed FIS controller.

This capacity is incremented here by augmenting the number of SMES devices composing the DES system. In both cases, two appropriate wind profiles digitalized during 600 s (10 min) were applied. The first one has a constant mean value of the wind speed at about 10 m/s, and the second one has a variable mean value of the wind speed, so that it makes the wind generator to operate near to the maximum and minimum power. Both employed wind speed profiles are shown in Figs. 8.

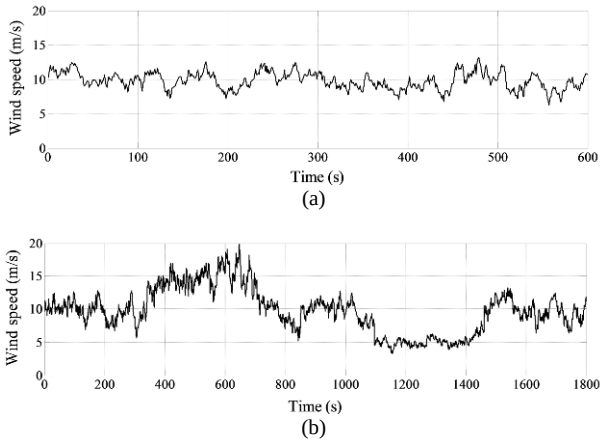

Figs. 8. Wind speed with different mean values: (a) Constant (10 m/s) and (b) Variable

The value of the dead-band width for the backlash block is adjusted based on the maximum variation of wind power, $\Delta P_{wg,\,max}$ around its mean value, $P_{wg,\,mean}$ (which is related to the mean value of the wind speed, $W_{s,\,mean}$) and the maximum capacity of the energy storage device. In this application, the values of the dead-band width for the backlash block were obtained based on simulations and test for different mean wind speeds and for different number of storage devices. The tests were performed with 1, 2 and 4 SMES devices (approximately half, same and twice, respectively, the power of the wind generator used in the case studies). Table II shows the values obtained from these tests, which are used for the case studies subsequently presented. In operation, the dead-band width adopted is set according to the mean wind speed in three speed ranges (0-4, 5-12 and 13-25 m/s).

TABLE II
DEAD-BAND WIDTH ADOPTED FOR DIFFERENT MEAN VALUES OF WIND SPEED AND VARIOUS NUMBER OF SMES DEVICES

$W_{s,\,mean}$	$P_{wg,\,mean}$	$\Delta P_{wg,\,max}$	Dead-band (DB) width (kW)		
(m/s)	(kW)	(kW)	1 SMES	2 SMES	4 SMES
4	36	180	48	84	144
6	240	672	480	840	1440
8	600	960			
10	1164	1080			
12	1596	888			
14	1728	432	48	84	144
16	1740	312			
18	1745	96			
20	1747	96			
22	1746	96			
24	1746	96			

IV.1. Scenario 1: Assessment of the Dynamic Performance of the Proposed Active Power Control of the SMES. Comparison with Another Efficient Control

In this scenario, simulations are carried in order to assess the dynamic performance of the proposed FIS active power control of the SMES in comparison with the method based on [20]. In this last novel technique, the APC yields the regulating power, P_{reg} by processing

the wind power generation, P_{reg} using a fixed structure architecture controller, also called multi-band structure (MBS), as shown in Fig. 9. This new controller achieves a robust tuning over a wide range of frequency variations while keeps the same structure. It separates the frequency spectra of input signals in decoupled bands for covering various signal frequency variations. This controller is employed since authors claimed that it ensures fast controllability of the SMES operating in the four-quadrant modes, and enables to effectively increase the transient and dynamic stability of the microgrid. However, as can be noted from inspection of Fig. 9, the SMES coil current is not used as input, so that the MBS controller does not take into account the state-of-charge of the energy storage and aims at achieving just the better control action as if the storage capacity were sufficient for any application. Simulations are done with the connection at bus 6 of a SMES system composed of 2 shunt-connected SMES devices.

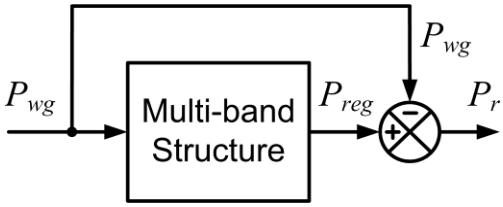

Fig. 9. General structure of the active power controller implemented with the MBS controller proposed in [22] for compensating wind power fluctuations

IV.1.1. Case A: Constant Mean Wind Speed

In this study, the wind speed profile applied to the wind power generator is shown in Fig. 8(a) is. The active power injected by the WPG, P_{wg}, for these wind speed variations is shown in Fig. 10(a).

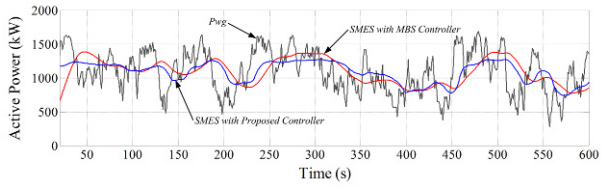

(a)

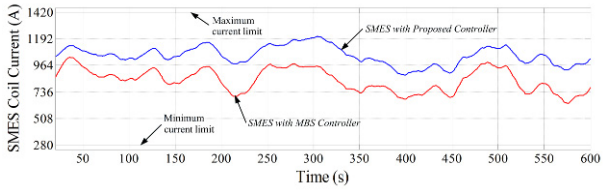

(b)

Figs. 10. Dynamic response of the wind generator for the case with constant mean wind speed (scenario 1 - case A): (a) Active power injected into the MG by the WPG, and the WPG-SMES with both the proposed FIS controller and the MBS controller. (b) SMES coil current with both the proposed FIS controller and the MBS controller

The active power injected into the MG by the WPG plus the SMES system (2 SMES devices) is also shown in the same figure, with the proposed FIS active power control method (*SMES with Proposed Controller*), and the other method, i.e. the multi-band structure controller (*SMES with MBS Controller*). The performance of the SMES coil current (state-of-charge) for one of the SMES devices is shown in Fig. 10(b) with both control methods.

It can be observes that, with the proposed method and the control with *MBS Controller*, the output power fluctuations of the whole system are significantly reduced, and the coil current never falls below the minimum current limit (uncharged state) and does not exceed the maximum current (overcharged state).

This is a consequence that the energy storage system is slightly demanded, so that the influence of the SMES state-of-charge is very low.

IV.1.2. Case B: Variable Mean Wind Speed

Now, the wind speed profile shown in Fig. 8(b) is applied to the wind power generator. In this case the storage device is quite more required than the previous case. The active power injected by the WPG, P_{wg} and by the WPG plus SMES (combined WPG-SMES system) with *Proposed Controller* and *MBS Controller* are shown in Fig. 11(a).

The performance of the superconducting coil current for one of the SMES devices of the system is shown in Fig. 11(b) for the two control methods.

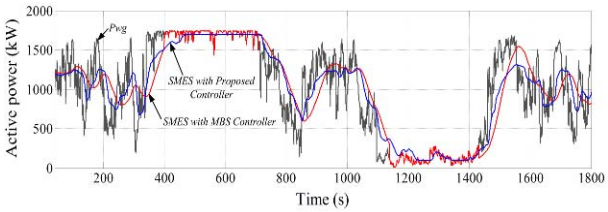

(a)

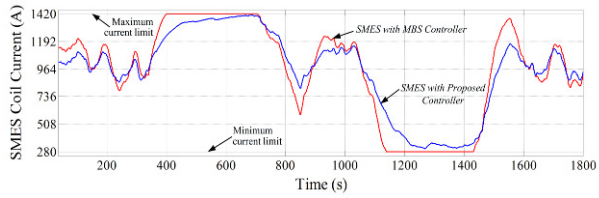

(b)

Figs. 11. Dynamic response of the wind generator for the case with variable mean wind speed (scenario 1 - case B): (a) Active power injected into the MG by the WPG, and the WPG-SMES with both the proposed FIS controller and the MBS controller. (b) SMES coil current with both the proposed FIS controller and the MBS controller

It can be noted that the energy storage device with *MBS Controller* reaches its lower and upper limits and the controller loses the regulation capacity, as expected since this controller does not include the SMES coil current as a control input.

This method could operate properly when the storage capacity is rather large and therefore not optimized.

As can be also seen, with the same storage capacity, the proposed FIS method smoothes the wind power fluctuations without reaching any limit.

Therefore, the proposed method could counteract the wind power fluctuations with less storage capacity than that used by the other method.

IV.2. Scenario 2: Assessment of the Dynamic Performance of the Proposed Active Power Control of the SMES with Different Storage Capacities

In this scenario, simulations are made considering different storage capacities of the SMES system with the proposed FIS controller. To this aim, various SMES systems are evaluated, composed of 1, 2 and 4 SMES devices connected in parallel at the same feeder (PCC). In this way, the studied SMES systems correspond to approximately half, the same and twice, respectively, the active power of the WPG. As in the previous scenario, all simulations were carried out with constant and variable mean wind speed in order to assess the dynamic performance of the proposed SMES active power control.

IV.2.1. Case A: Constant Mean Wind Speed

In this study, the wind speed profile with constant mean value of 10 m/s, shown in Fig. 8(a), is applied to the wind power generator. The active power injected by the WPG, P_{wg} and by the WPG plus SMES (combined WPG-SMES system) with 1, 2 and 4 devices for this wind profile is shown in Fig. 12(a). The performance of the superconducting coil current for one of the SMES devices of the system is shown in Fig. 12(b).

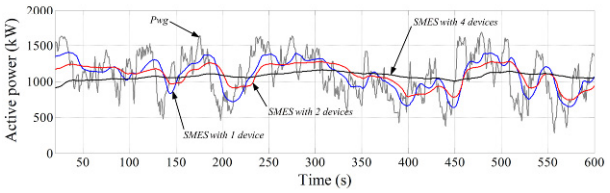

(a)

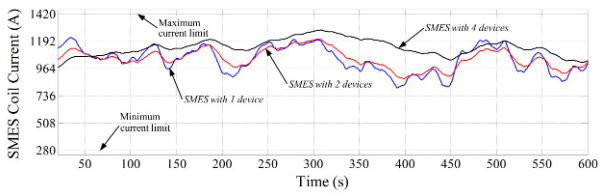

(b)

Figs. 12. Dynamic response of the wind generator for the case with constant mean wind speed (scenario 2 - case A): (a) Active power injected into the MG by the WPG, and the combined WPG-SMES system consisted of 1, 2 and 4 SMES devices. (b) Coil current of the SMES system composed of 1, 2 and 4 SMES devices

As can be noted, the higher the number of SMES devices composing the SMES system, the better the counteracting of the power fluctuations injected by WPGs.

IV.2.2. Case B: Variable Mean Wind Speed

For the case with variable mean wind speed, the wind speed profile shown in Fig. 8(b) is applied to the WPG. In this case the energy storage device is more required than the previous case. The active power injected by the WPG, P_{wg} and by the WPG plus SMES with 1, 2 and 4 devices for the variable mean wind speed is shown in Fig. 13(a). The dynamic performance of the superconducting coil current for one of the SMES devices is shown in Fig. 13(b) for this case.

It can be observed from Figs. 12 and Figs. 13 that the controller with the proposed control responds effectively reducing the wind power fluctuations, preventing that these large fluctuations impact to the microgrid. The figures show also that the higher the number of SMES devices and therefore larger the resulting energy storage capacity, the greater the smoothing effect of the output power. Moreover, using the proposed FIS control system, the coil current never falls below the minimum current limit (uncharged state) and does not exceed the maximum current limit (overcharged state) in all cases.

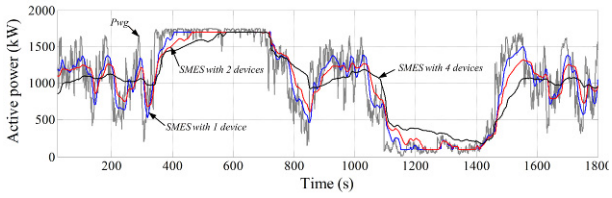

(a)

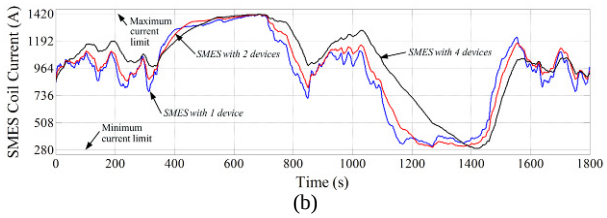

(b)

Figs. 13. Dynamic response of the wind generator for the case with variable mean wind speed (scenario 2 - case B): (a) Active power injected into the MG by the WPG, and the combined WPG-SMES system consisted of 1, 2 and 4 SMES devices. (b) Coil current of the SMES system composed of 1, 2 and 4 SMES devices

V. Conclusion

This paper has proposed an effective SMES controller for stabilizing the active power fluctuations injected into the AC microgrid by wind generators. The design and implementation of a high performance active power controller of the SMES has been presented. The multi-level control proposal is designed in the synchronous-rotating *d-q* reference frame. It is based on fuzzy logic

techniques and uses an improved fuzzy inference system (FIS) combined with a unique filter block. Moreover, the detailed model of the SMES unit and its power conditioning system for connecting to the microgrid has been studied. The dynamic performance of the proposed system and its impact on the MG operation in grid-interactive operation has been fully validated by computer simulation.

The results show that the novel multi-level control scheme ensures fast controllability of the SMES operating in the four-quadrant modes, which enables to charge/discharge the SMES in a fast and very controlled manner. The SMES system can effectively compensate the active power fluctuations from a WPG and hence can improve the power quality and reliability of the AC microgrid.

The complete system (WPG plus SMES) generates a smoother power response than that of the system without the DES system. This compensating effect of the output power increases with the number of devices composing the SMES system. Finally, it can be concluded that the active power control proposed for the SMES achieves a very good management of the energy stored, counteracting wind power fluctuations while preventing the device from becoming overcharged or uncharged.

Acknowledgements

This work was supported by the CONICET (Argentinean National Council for Science and Technology Research), the ANPCyT (Argentinean National Agency for Scientific and Technological Promotion) and the National University of San Juan (UNSJ) under Grant PICTO−UNSJ 2009, No. 0162.

References

[1] R. Diabi, N. Belizidia, Distributed Generation Influence on the Electric Network Voltage Level, *International Review of Electrical Engineering (IREE), vol. 3 n. 2*, 2008, pp. 242-247.

[2] J.M. Guerrero, F. Blaabjerg, T. Zhelev, K. Hemmes, E. Monmasson, S. Jemei, M.P. Comech, R. Granadino, J.I. Frau, Distributed Generation: Toward a New Energy Paradigm, *IEEE Industrial Electronics Magazine*, *vol. 4 n. 1*, March 2010, pp. 52-64.

[3] B. Kroposki, R. Lasseter, T. Ise, S. Morozumi, S. Papatlianassiou, N. Hatziargyriou, Making Microgrids Work. *IEEE Power & Energy Magazine*, *vol. 6 n. 3*, May/June 2008, pp. 40-53.

[4] M. Wissner, The Smart Grid – A Saucerful of Secrets? *Applied Energy*, *vol. 88 n. 7*, July 2011, pp. 2509-2518.

[5] A. Ali Reza, S. Ali Reza, The Basic Concepts of Smart Grid: Initiatives, Technologies, Characteristics, Standards and Solutions, *International Review of Electrical Engineering (IREE)*, *vol. 3 n. 1*, 2010, pp. 64-69.

[6] N. Hatziargyriou, H. Asano, R. Iravani, C. Marnay, Microgrids, *IEEE Power & Energy Magazine*, *vol.5 n. 4*, 2007, pp. 78-94.

[7] M. Hamidreza, S. Seyedmohamad, E. Mohamadreza, Microgrids Control in Islanding Mode Operation considering a Hybrid Model of Distributed Generation Units of Wind and Fuel Cell, *International Review of Electrical Engineering (IREE), vol. 4 n. 1*, 2011, pp. 188-195.

[8] F. Katiraei, R. Iravani, N. Hatziargyriou, A. Dimeas, Microgrids Management: Controls and Operation Aspects of Microgrids, *IEEE Power & Energy Magazine*, *vol. 6 n. 3*, 2008, pp. 54-65.

[9] B.V. Mathiesen, H. Lunda, K. Karlsson, 100% Renewable Energy Systems, Climate Mitigation and Economic Growth, *Applied Energy*, *vol. 88 n. 2*, 2011, pp. 488-501.

[10] S. Skander-Mustapha, M. Jebali-Ben Ghorbal, J. Arbi, I. Slama-Belkhodja, Comparative Analysis of Control Strategies for DFIG Based Wind System under Small Grid Faults, *International Review of Electrical Engineering (IREE), vol. 4 n. 6*, 2009, pp. 1273-1282.

[11] I. Serban, C. Marinescu, Power Quality Issues in a Stand-Alone Microgrid Based on Renewable Energy, *Revue Roumaine des Sciences Techniques – Série Électrotechnique et Énergétique*, *vol. 53 n. 3*, 2008, pp. 285-293.

[12] Y. Hoseynpoor, T. PirzadehAshraf, Sh. Sajedi, T. Karimi, Evaluation of Power Quality in a Wind Power Generation System, *International Review of Electrical Engineering (IREE), vol. 4 n. 3*, 2011, pp. 1233-1238.

[13] M.G. Molina, *Emerging Advanced Energy Storage Systems: Dynamic Modeling, Control and Simulation* (Nova Science Publishers, Inc., 2012).

[14] M.V. Aware, D. Sutanto, Improved controller for Power Conditioner Using High-Temperature Superconducting Magnetic Energy Storage (HTS-SMES), *IEEE Trans. on Applied Superconductivity*, *vol.13 n..1*, 2003, pp. 38-47.

[15] M.G. Molina, P.E. Mercado, E.H. Watanabe, Static Synchronous Compensator with Superconducting Magnetic Energy Storage for High Power Utility Applications, *Energy Conversion and Management*, *vol. 48 n. 8*, 2007, pp. 2316-2331.

[16] M.H. Ali, T. Murata, J. Tamura, Transient Stability Enhancement by Fuzzy Logic-controlled SMES Considering Coordination with Optimal Reclosing of Circuit Breakers, *IEEE Trans. on Power Systems*, *vol. 23 n. 2*, 2008, pp. 63-640.

[17] S. Dechanupaprittha, K. Hongesombut, M. Watanabe, Y. Mitani, I. Ngamroo, Stabilization of Tie-Line Power Flow by Robust SMES Controller for Interconnected Power System With Wind Farms, *IEEE Trans. on Applied Superconductivity*, *vol. 17 n.2*, 2007, pp. 2365-2368.

[18] M.G. Molina, P.E. Mercado, E.H. Watanabe, Improved Superconducting Magnetic Energy Storage (SMES) Controller for High Power Utility Applications, *IEEE Trans. on Energy Conversion*, *vol. 26 n. 2*, 2011, pp. 444-456.

[19] S. Vazquez, S.M. Lukic, E. Galvan, L.G. Franquelo, J.M. Carrasco, Energy Storage Systems for Transport and Grid Applications, *IEEE Trans. on Power Electronics*, *vol. 57 n. 12*, 2010, pp. 3881-3895.

[20] M.G. Molina, P.E. Mercado, Power Flow Stabilization and Control of Microgrid with Wind Generation by Superconducting Magnetic Energy Storage, *IEEE Trans. on Power Electronics*, *vol. 26 n. 3*, 2011, pp. 910-922.

[21] M. S. Majid, M. Y. Hassan, H. A. Rahman, Damping Power System Oscillations Using Superconducting Magnetic Energy Storage for Single Machine Infinite Bus, *International Review of Electrical Engineering (IREE)*, *vol. 4 n. 2*, 2011, pp. 739-744.

[22] M.G. Molina, P.E. Mercado, E.H. Watanabe, Analysis of Integrated STATCOM-SMES based on Three-Phase Three-Level Multi-Pulse Voltage Source Inverter for High Power Utility Applications, *Journal of the Franklin Institute*, *vol. 348 n. 9*, November 2011, pp. 2350-2377.

[23] M.H. Ali, B. Wu, R.A. Dougal, An Overview of SMES Applications in Power And Energy Systems, *IEEE Trans. Sustainable Energy*, *vol. 1 n. 1*, 2010, pp. 38-47.

[24] L. Chen, Y. Liu, A.B. Arsoy, P.F. Ribeiro, M. Steurer, M.R. Iravani, Detailed modeling of Superconducting Magnetic Energy Storage (SMES) System, *IEEE Trans. on Power Delivery*, *vol.21 n. 2*, April 2006, pp. 699-710.

[25] T.T. Ma, Advanced Control Techniques for Grid-connected Distributed Generators in Microgrids, *International Review of Electrical Engineering (IREE)*, *vol. 5 n. 6*, 2010, pp. 2764-2772.

[26] A.A. Salam, A. Mohamed, M.A. Hannan, H. Shareef, An Improved Inverter Control Scheme for Managing the Distributed

Generation Units in a Microgrid, *International Review of Electrical Engineering (IREE), vol. 5 n. 3*, 2010, pp. 891-899.
[27] E. Cox, Fuzzy Fundamentals, *IEEE Spectrum, vol. 29 n. 10*, October 1992, pp. 58-61.
[28] G. Tao, P.V. Kokotovic, Adaptive Control of Systems with Backlash, *Automatica, vol. 29 n. 2*, 1993, pp. 323-335.
[29] E.H. Mamdani, S. Assilian, An Experiment in Linguistic Synthesis with a Fuzzy Logic Controller, *International Journal Man-Machine Studies, vol. 7 n 1*, 1975, pp. 1-13.
[30] L.H. Tsoukalas, R.E. Uhring, *Fuzzy and Neural Approach in Engineering* (John Wiley and Sons, Inc., 1987).
[31] The MathWorks Inc. SimPowerSystems for Use with Simulink: User's Guide, 2012. Available: http://www.mathworks.com/.

Authors' information

CONICET, Instituto de Energía Eléctrica, Universidad Nacional de San Juan, San Juan, Argentina.

Marcelo G. Molina graduated summa cum laude as Electronic Engineer from the National University of San Juan (UNSJ), Argentina, in 1997, and received the Ph.D. degree from the UNSJ in 2004. During 2004, he was a Doctoral Research Fellow at the Federal University of Rio de Janeiro, Brazil, supported by CAPES. From 2005 to 2007, he worked as a Post-Doc Research Fellow from the Argentinean National Council for Science and Technology Research (CONICET) at the Institute of Electrical Energy (IEE), UNSJ. In 2009, he was a Visiting Professor at the University of Siegen, Germany, sponsored by DAAD, and in 2010 at the Federal University of Rio de Janeiro, Brazil, supported by CAPES. In 2004, he became an Assistant Professor with tenure at the UNSJ, and he was promoted to Associate Professor of Electrical Engineering in 2011. Since 2008, Dr. Molina is an Associate Researcher of the CONICET and in 2011 he became Deputy Director of the IEE at the UNSJ. His research interests include, power system modeling, analysis and control, power electronics and electrical drives, microgrid and smart grid technologies and distributed energy resources with emphasis on distributed and renewable generation and the grid-interactive application of energy storage.
He has been involved in many national and international research projects and in high-level consulting with the industry. He is the author or coauthor of more than 130 publications in his research fields including ISI/SCOPUS journal and conference proceeding papers, books and book chapters.
Dr. Molina a member of the IEEE Power Engineering Society, the IEEE Power Electronics Society and the Brazilian Power Electronics Society (SOBRAEP), among others.

Gastón O. Suvire was born in San Juan, Argentina. He graduated as an electric engineer from the National University of San Juan (UNSJ), Argentina in 2002. He received his Ph.D. from the same university in 2009, carrying out part of his doctorate in the COPPE institute, at the Federal University of Rio de Janeiro in Brazil, supported by CAPES. From 2009 to 2011, he worked as a Post-Doc Research Fellow from the Argentinean National Council for Science and Technology Research (CONICET) at the Institute of Electrical Energy (IEE), UNSJ. He is currently an Assistant Professor of Electrical Engineering at the UNSJ. His research interests include simulation methods, power systems dynamics and control, power electronics modeling and design, and the application of wind energy and energy storage in power systems.

Pedro E. Mercado was born in San Juan, Argentina. He graduated as electromechanical engineer from the UNSJ, and received his Ph.D. from the Aachen University of Technology (RWTH), Germany. He is currently Full Professor with tenure of Electrical Engineering at the UNSJ and an Associate Researcher of the CONICET. His research activities focus on operation security, power electronics, renewable energy systems, and economic operation and control of electric power systems.
Dr. Mercado is a Senior Member of the IEEE Power Engineering Society and the Power Electronics Society.

